Published in Composites Science and Technology 90 (2014) 1–8
DOI: 10.1016/j.compscitech.2013.10.010

Effect of High Through-Thickness Compressive Stress on Fibre Direction Tensile Strength of Carbon/Epoxy Composite Laminates

Khong Wui Gan, Michael R. Wisnom, Stephen R. Hallett*

Advanced Composites Centre for Innovation and Science, University of Bristol, University Walk, Bristol, BS8 1TR, United Kingdom.

* Corresponding author. Tel.: +44 (0)117 33 15504. E-mail address: Khong.Wui.Gan@bristol.ac.uk.

Abstract

The fibre-direction tensile strength of carbon/epoxy laminates under the influence of through-thickness compressive stresses has been experimentally investigated. In a unidirectional (UD) laminate, the through-thickness compressive stresses will cause premature longitudinal fibre-splitting, masking the effect of transverse stresses on the fibre-direction strength. Here a cross-ply laminate has been used. With the addition of 90° plies preventing the 0° fibres from splitting, it effectively allows the dependence of fibre-direction tensile strength on high through-thickness stresses to be studied. The severity of the through-thickness loads has been varied using cylindrical indenters of different radii, up to the loads near the through-thickness compressive failure stress of the cross-ply laminate. The results show that there is a linear decrease in fibre-direction strength with the mean through-thickness stress. In all the test cases, the specimens failed in a catastrophic brittle manner, with scanning electron micrography showing primarily a fibre tensile fracture mode. The detailed stress state in the specimens has been calculated via finite element analysis. Two failure criteria are proposed, which can be used as conservative design criteria concerning fibre-dominated failures in multiaxial load scenarios.

Keywords: A. Polymer-matrix composites (PMCs); B. Strength; C. Failure criterion, finite element analysis (FEA)

Published in Composites Science and Technology 90 (2014) 1–8
DOI: 10.1016/j.compscitech.2013.10.010

1.0 Introduction

With the increasing use of composite materials replacing metals in aerospace applications, the need to consider complex load conditions is also increasing. Highly localised through-thickness stresses can often be seen in components where localised contact conditions exist, such as in bolted joints. These stresses may interact with co-existing primary in-plane tensile loading in the fibre-direction, leading to earlier failure.

Multiaxial stress problems in composites have gained attention through efforts such as the Worldwide Failure Exercises (WWFE-I and II) [1, 2]. However there is still a paucity of reliable experimental data for biaxial or multiaxial load cases, especially for those involving through-thickness compression and in-plane tension, due to the cost and complexity of multiaxial testing. A number of works have investigated the unidirectional tensile strength of composites under hydrostatic pressure [3-9]. The results of these studies show that the strength and the failure mode of composites depend strongly on the magnitude of the hydrostatic pressure. There is a general trend of decreasing longitudinal tensile strength with increasing pressure.

Works by Collings [10] compared the differences between transverse compressive failures in unconstrained and constrained conditions for unidirectional carbon fibre reinforced composites. The failure modes are totally different, i.e. in the unconstrained case the planes of failure are always parallel to the fibres (inter-fibre failure), whereas the specimens in a transversely constrained condition fail on planes parallel to the direction of constraint in which the failure mode is shear through the fibres caused by the resolved shear stress component of the applied load. Similar observations were also obtained by Henriksson [11] when he studied through-thickness compressive loading on unidirectional and cross-plied carbon/epoxy AS4/8552 laminates.

The through-thickness stresses that interact with the unidirectional composite fibre direction strength found in the literature are mostly in the form of hydrostatic pressure, at most up to moderate values of ~700 MPa. The current study is a detailed expansion of initial results presented in [12]. In this work, a biaxial test method is developed to apply highly localised through-thickness compressive stress (locally as high as -1700 MPa, as calculated by linear elastic finite element analysis) on a simple cross-plied carbon/epoxy tensile test specimen. The high through-thickness compressive strength of a cross-plied laminate allows the interaction between a broad range of through-thickness compression and in-plane tensile strength to be examined. Multiple experimental load cases are presented and finite element models have been used to study the stresses within the specimens so that a simple failure criterion can be proposed for engineering design purposes.

2.0 Experimental

2.1 Specimen preparation and rig setup

The material under consideration is Hexcel's carbon epoxy pre-preg system, IM7/8552 with a nominal ply thickness of 0.125 mm. Four identical panels with a cross-ply stacking sequence of $[(0/90)_7/0/(90/0)_7]$ were fabricated, from which specimens were cut for the various load cases. The actual thickness of the laminates is 3.63 mm. The 0° direction refers to the longitudinal tensile loading direction. The 90° plies were present to prevent the specimens from splitting transversely due to the high through-thickness compressive loading. The laminates were cured according to the manufacturer's specification. In order to avoid damage due to mechanical gripping, end tabs 100 mm long, made of cross-plied glass/epoxy, were glued to both ends of the panel, leaving a 100 mm-long untabbed gauge section. Specimens of 10 mm width (Figure 1d) were cut from it using a water-cooled diamond wheel cutter. For accurate stress calculation, the width and thickness of every specimen was measured.

The tests were performed using a Zwick/Roell 100 kN tension/compression biaxial testing machine, equipped with four independent hydraulic grips mounted horizontally on a flat steel base (Figure 1a). One pair of actuators was in the longitudinal direction while the other pair was in the perpendicular through-thickness direction. Both the displacement and load could be monitored independently for all four actuators. Since the longitudinal actuators could not be brought very close together due to the presence of the transverse actuators, custom designed fixtures and jaws were manufactured from EN24 high tensile steel to hold the specimens (Figure 1b). For gripping and applying the tensile load on the specimens, two pairs of clamps were built with knurled surfaces to enhance friction. Four M8 high tensile bolts were used for tightening each clamp at 40 Nm of torque. The clamps were each connected to the hydraulic grips on the longitudinal actuators with a steel extension rod via an M20 bolt.

Highly localised through-thickness compressive loading was applied via a pair of heat-treated steel (BS4659 B01) indenters with different radii of curvature. Four different radii (R = 10 mm, 20 mm, 40 mm and 80 mm) were used to give different severity of the localised through-thickness compression. A spirit level was used to ensure good horizontal alignment of all the extension rods and the indenters. A high speed camera was set up from the top (Figure 1a) to capture the instant of failure at 216,000-300,000 fps.

2.2 Test procedures

After the specimen was clamped in position, one of the transverse indenters was brought in until it just touched the specimen and was locked in position (i.e. in a displacement control mode). The other was then set in load control and the through-thickness compressive load applied at a rate of 1 kN/s. Note that in load control mode, load is the prescribed quantity and the resulting displacement is a function of specimen compliance. There was no noticeable

bending due to this slightly asymmetric loading arrangement as there were two M20 bolts (Figure 1b) that allowed transverse movement and the specimens were sufficiently long. This was confirmed upon checking the negligible difference in load readings between the two opposite hydraulic actuators. After the compressive load stabilised, both the longitudinal actuators loaded the specimen under displacement control, each at a nominal rate of 0.5 mm/min simultaneously to preserve the symmetry of the loading condition and also to minimise the influence of friction between the indenters and the specimen. The specimen was loaded until catastrophic failure.

The through-thickness compression in load control mode would tend to crush and obliterate any features of the fracture surface as soon as the specimen failed in tension. Therefore 8 additional specimens were loaded in displacement control with indenters of R = 20 mm so that the fracture surfaces could be preserved and inspected. Two additional specimens were also loaded purely in through-thickness compression with indenters of R = 10 mm but without a longitudinal mechanical grip (Figure 1c), to check if the end restraints had any effect. The failure surfaces were then examined in a scanning electron microscopy (SEM).

For validation of the finite element models later, the experimental contact areas under the indenters were measured for two extra specimens of each load case. The contact area was identified by marking the area adjacent to the indenters with quick-dry acrylic paint whilst under through-thickness compressive load only (inset of Figure 2). It was assumed that the material deformation was small enough so that the contact area marked during the test and measured after the test would not be significantly different.

2.3 Results

In a cross-ply laminate, the majority of the longitudinal tensile load will be carried by the 0° plies. In the experiment, all specimens failed instantaneously by tensile failure in the 0° plies

without any sign of damage or load drop in the course of loading. The test results are summarised in Table 1. Each value in the table is an average of between three and five tests. There is a significant reduction of longitudinal tensile strength with through-thickness compressive loads. Note that the 40 kN compression of indenter R = 10 mm corresponds almost to the load required to fail the specimens in the through-thickness direction, which is about 42 kN.

To have a meaningful representation of all the load cases of different indenter radii in a single laminate level failure envelope, the corresponding failure loads need to be normalised and presented as stresses. The fibre direction stresses in the 0° plies were simply calculated from the longitudinal tensile failure loads using classical laminate theory (CLT) and the measured dimensions. The unidirectional ply elastic properties for IM7/8552 carbon/epoxy in the conventional principal material axes are taken from [13]: E_{11} = 161 GPa, $E_{22} = E_{33}$ = 11.4 GPa, $\nu_{12} = \nu_{13}$ = 0.32, ν_{23} = 0.435. Residual thermal stresses were ignored for this analysis as they were small compared to the failure stresses in the fibre-direction. The through-thickness compressive loads were normalised as mean compressive stresses on the specimens by dividing the loads by the measured contact areas. Although the peak compressive stresses under the indenters were higher than the mean, the latter can be directly measured from the experiment. The results thus obtained are shown in Figure 2. The error bars show the standard deviation of measured strengths calculated from CLT. The unidirectional fibre-direction tensile strength (2724 MPa) obtained from the Hexcel datasheet [14] is plotted as a dashed line for comparison.

No experimental data could be obtained for mean compressive stresses below 300 MPa as the specimens tend to fail in tension at the end tabs due to the stress concentration. Beyond the mean compressive stress of 300 MPa, a linear decreasing trend (drawn using the data from the load control specimens only) of the fibre-direction strength is observed down to zero at a

through-thickness compressive stress of 1200 MPa, close to the through-thickness strength of the laminate. From the pure through-thickness compressive tests with 10 mm radius indenters, an average of compressive load at failure of 42 kN was measured. No load drop was observed until sudden failure of the specimens. However the contact area cannot be measured for this case and therefore the mean stress cannot be determined. A linear elastic finite element analysis with contact shows that the compressive load at failure corresponds to a mean stress of 1300 MPa. Note that the peak stress underneath the indenter is -1700 MPa, showing that the actual through-thickness compressive strength is higher than 1300 MPa. Knowledge of the mean compressive stress in conjunction with the above failure envelope allows the failure stress in a cross-plied laminate to be predicted under similar loading conditions. The mean compressive stress can be estimated using Hertzian contact analysis, and a more accurate approximation of the load-contact area relation taking into account the finite thickness of the specimen is given in [15].

A carbon/epoxy composite unidirectional lamina, if constrained in the transverse direction, can have a surprisingly high through-thickness compressive strength. A similar order of magnitude of high through-thickness compressive strength has also been reported for a small 7×7×6.4 mm AS4/8552 cross-ply laminate [11], which was measured as 1215 MPa. The compressive tests were performed with a flat surface and nearly all specimens failed with a fracture surface 30° to the loading direction. The actual strength could be higher and the appearance of this shear failure mode is perhaps due to the proximity of the failure initiation point to the free edges of the small specimens. This is supported by another experiment in the same reference [11] which reported that the through-thickness compressive strength of a transversely constrained (in the 2-direction) unidirectional specimen of the same material exceeded 1960 MPa, beyond the 100 kN loading capability of the test machine, and yet exhibited no failures. The very high compressive strength obtained in the present study is

attributed to the transverse constraint of the 90° plies, without which longitudinal splitting in the fibre direction would occur (Figure 3a).

Another interesting point is that, when a best fit line is drawn through the experimental points in Figure 2 and extrapolated to the y-axis, it shows an expected fibre-direction strength of a 0° lamina of about 3200 MPa. This value is close to the tensile strength of 3131 MPa for 1 mm^3 of IM7/8552, derived from scaled unidirectional tests based on Weibull strength-volume scaling [16]. The lower value of 2724 MPa reported in the manufacturer datasheet [14] is probably due to the test specimen size effect or an underestimate of the true strength due to the effect of stress concentrations at the tabs.

2.4 Failure surface inspection

Macroscopically, all the failure surfaces show brittle fibre failure with a clean and flat fracture surface perpendicular to the longitudinal direction of the specimen. The moment of failure captured by the high speed camera for one of the load cases (Figure 3b) shows that the failure occurs catastrophically on the symmetry plane underneath the peak pressure of the indenters, breaking the specimens symmetrically into halves. However, it is not possible to tell exactly where the failure initiated on the failure plane from the high speed images as the fracture happens too quickly with the frame before it showing an essentially intact specimen.

Under load control the indenters induced additional crushing damage to the fracture surface after failure, hindering subsequent surface inspection. Therefore eight specimens were loaded in displacement control with indenters R = 20 mm. Compressive loads reduced slightly due to the Poisson's contraction from the tensile loading, and the values at final failure were recorded. These experimental points are also shown in Figure 2, with the mean through-thickness compressive stress calculated using the force-contact area relation proposed in [15] rather than from measured contact areas. These show a good match to the load control data.

Figure 3c shows the fracture surface of a specimen under low through-thickness compression at 17.6 kN in displacement control, whereas Figure 3d corresponds to a fracture surface subjected to high through-thickness compression of 50.3 kN, also in displacement control. In both figures, the specimens show primarily a flat fracture surface perpendicular to the longitudinal direction, except that crushing damage can be seen on the specimens subjected to high through-thickness compression despite being loaded in displacement control. It is not clear if this damage happened before, during or after ultimate failure.

Failed unidirectional specimens in uniaxial tension will often exhibit a broom-like failure surface with significant fibre pull-out due to random fibre bundle fracture [3-5, 7]. However when the uniaxial tensile loading is superimposed with hydrostatic pressure, it gives a clean and almost flat fracture surface [3-5, 7]. This is also true for the cross-ply specimens under biaxial through-thickness compression and in-plane tension considered here. The additional constraint imposed by the adjacent 90° plies creates a compressive state of stress in both the transverse directions which prevents any longitudinal splitting in the 0° plies, leading to a tensile fibre failure mode.

Even in the pure through-thickness compressive load case with indenters R = 10 mm, at 42 kN compressive failure load, the specimens appear to fail primarily by tensile fibre failure mode in the 0° plies. This is seen in the SEM images of the corresponding fracture surface in Figure 4. At the free edge of the specimen, some localised fibre failure that is distinctively different from the rest can be seen. This can be attributed to the bending stress (due to the material being squeezed out as a result of the high through-thickness compression and lack of constraint at the edge) as well as the highly-localised interlaminar shear stress (due to ply property mismatch) at the free edge [17]. In Figure 4a, the plies near to the surface were actually crushed into debris by the indenters and fell off. The 0° plies in the middle of the

specimen, which are far from the crushing damage, could still be inspected. This is given in Figure 4b, which shows a clear tensile fibre failure mode.

3.0 Numerical

3.1 Finite element (FE) model

The macroscopic laminate level failure envelope in Figure 2 is based on average stresses and so is mainly of use for practical engineering solutions. It is also instructive to look at the local interaction of stresses at the ply level so that a stress-invariant meso-scale level failure criterion can be sought. A further question remains as to where the failure initiates on the facture plane and what combination of stresses causes the failure. Here the highly complex stress fields within the specimens at failure are calculated numerically using finite element (FE) analysis. From the SEM image of the most severe pure through-thickness compression load case in Figure 4a, the free edge damage is locally confined to the free edge, leaving a large portion of the specimen width under high triaxial stresses. Based on this observation, and also from the consideration that there is transverse constraint imposed by the 90° plies, the problem can be approximated as a 2D problem assuming plane strain across the width.

Due to geometrical and loading symmetry, only a quarter of the gauge section needed to be analysed. It was meshed with fine elements (element length about 0.013 × 0.016 mm, 8 elements across each ply thickness) underneath the indenter and coarser elements further away. The smallest contact length of the load cases has been represented by at least 170 elements. The steel indenter was meshed with elements as fine as 0.035 mm. A nonlinear material model taking into account the effect of hydrostatic pressure was found not to show significant difference in the stresses on the symmetry (failure) plane compared to those computed using a linear model, as high hydrostatic compressive stresses are present in the specimen when loaded in through-thickness compression which prevents nonlinear yielding.

Published in Composites Science and Technology 90 (2014) 1–8
DOI: 10.1016/j.compscitech.2013.10.010

Fully-integrated Abaqus/Standard four-node plane strain CPE4 elements were thus used for both materials with linear elastic material properties. Geometric non-linearity was included. The unidirectional ply elastic properties for IM7/8552 carbon/epoxy are as given in Section 2.3 and the coefficients of thermal expansion are $\alpha_1 = 0$ (index *1* refer to fibre direction), $\alpha_2 = \alpha_3 = 3\times10^{-5}$ °C^{-1} [18]. The steel elastic properties $E = 200$ GPa and $\nu = 0.3$ are used for the indenter. Initial parametric studies showed that the effect of friction at the contact (friction coefficient = 0.3) only affected the longitudinal stresses in the surface plies. They could either be increased or decreased by the frictional stresses depending on the load cases, but were never larger than the longitudinal stresses in the central plies which were unaffected by the friction coefficient. Therefore a penalty-based frictionless surface-to-surface contact was used to model the interaction of the specimen with the steel indenters. Thermal residual stresses due to specimen cool down following the curing process ($\Delta T = -160$ °C) were included in the analysis. The through-thickness load was first applied by the steel indenter, followed by prescribed tensile load, which is the average experimental failure load, at the specimen end.

3.2 FE results and failure criterion

Only the stresses in the dominating 0° plies along the failure plane, which is a symmetry plane in the FE models, are of interest. On the symmetry plane, the out-of-plane shear stress is zero. Only the three principal stresses exist there: the maximum σ_I due to the longitudinal tension (= σ_1 or S_{11}), the intermediate σ_{II} due to the transverse constraint imposed by the plane strain boundary conditions (= σ_2 or S_{22}) and the minimum σ_{III} due to the through-thickness compression (= σ_3 or S_{33}). The failure criterion here derived is therefore a function of these three principal stresses.

The contact lengths predicted by the FE models (doubled from the half model) are on average within 5% smaller than those measured from the experiment (Table 1), with a maximum deviation of 12% (for a 0.4 mm difference) for cases where the contact area was small and the measurement was more difficult. The deviation gets significantly smaller as the contact area increases and the measurement uncertainty reduces. It can thus be assumed that the linear material model used will give sufficiently accurate results for the highly localised through-thickness stresses under the indenter. The thickness direction principal stress distributions along the failure plane at the experimental tensile failure loads for two biaxial load cases with indenter R = 10 mm are given in Figure 5a and b, at the lowest through-thickness compressive load of 15 kN and the highest of 40 kN. The stress distributions for other load cases are similar, and differ only in magnitude. Due to symmetry, the stress distribution is shown for the half thickness.

In the first loading stage where only the through-thickness compression is applied, the through-thickness compressive stress reduces gradually from the top surface in contact with the indenter to the mid-plane of the specimen. The first few 0° plies under the indenters are essentially in longitudinal compression due to the high Hertzian contact stresses. All the principal stresses, though unequal, are compressive. The 0° ply stresses then rapidly become tensile and reach a plateau value near the mid-plane of the specimen. On the contrary, the 90° plies are always in compression due to the Poisson's ratio mismatch between the adjacent plies when they are subjected to through-thickness compression. There are distinctive longitudinal stress drops corresponding to the 0°/90° ply interfaces.

During the second loading stage when the tensile stress is applied, a tensile stress field is superimposed on the previous stress field, lowering the longitudinal compressive stresses in the first few 0° plies. Depending on the load case they may become slightly tensile, as shown in Figure 5a. Tensile failure would not have initiated in these first 0° plies, as their

longitudinal tensile stresses are not as high as those in the middle 0° plies. In the extreme load case of 40 kN through-thickness compression (which is near to the ultimate through-thickness failure load of 42 kN) with indenter R = 10 mm, all the principal stresses in the first plies are compressive (Figure 5b), so tensile failure is even more unlikely to initiate there.

This implies that the failure is expected to initiate at the 0° plies in the middle, where the tensile stresses are the highest. The fibre failure criterion in the commonly used Puck's or Cuntze's theory [1, 2] assumes that the longitudinal strain or stress at failure under multiaxial loading is a constant as determined from a uniaxial test. However, the FE longitudinal stresses or strains at failure for all of the 16 load cases considered here do not show them to be constant. It is thus necessary to seek an appropriate failure criterion that accounts for this variation. Based on the work of other researchers [3-9], the transverse stresses have been shown to have a role to play in determining the fibre-direction strength of a lamina. So it can be deduced that the failure is likely to have happened at a material point with some maximal combination of the three principal stresses. The simplest combination of the stresses is the Tresca stress, which is the difference between the maximum and the minimum principal stresses, i.e. $\sigma_I - \sigma_{III}$, where the contribution of the intermediate σ_{II} is ignored. We initially investigate if fibre failure occurs where the Tresca stress reaches a critical value, A:

Fibre failure Criterion A: $$\sigma_I - \sigma_{III} = A \quad (1)$$

where A is a material constant which can be measured from a simple mechanical test such as a uniaxial longitudinal tensile test.

The Tresca stress criterion however excludes the contribution of the intermediate principal stress, σ_{II}. In fact, it is important as the present study of the effect of through-thickness compressive stress on fibre direction strength shows the constraint provided by the transverse compressive σ_{II} stops the laminae from longitudinal splitting. As a complementary

examination, it is instructive to include it in the formulation of the fibre failure criterion. By giving equal importance to both the transverse principal stresses, σ_{II} and σ_{III}, a simplest modification to the original Tresca stress criterion in Equation (1) can be proposed:

Fibre failure Criterion B: $$\sigma_I - (\sigma_{II} + \sigma_{III}) = A \quad (2)$$

The 16 load cases presented here provide data to assess the two fibre failure criteria proposed above. The combination of stresses in Equations (1) and (2) are calculated at all nodes along the symmetry plane of the FE models for all load cases. They are illustrated in Figures 5c and d for two load cases of indenter R = 10 mm, also showing the location of the maximum values within the cross-plied specimens. Failure is expected to initiate where these maximum values are situated. They are extracted and plotted in Figure 6 against the mean through-thickness compressive stress. The fibre-direction tensile strength from the manufacturer [14] and the Weibull tensile strength of a small representative volume, 1 mm^3, for IM7/8552 [16] are also plotted as straight lines for comparison.

4.0 Discussion

In Figure 6, the maximum values of stress combination following both criteria mostly fall above the manufacturer's longitudinal tensile strength, which is probably an underestimate of the actual strength. This means that either one of them, by setting the material constant A to be the longitudinal tensile strength of a unidirectional ply, can be used as a conservative fibre failure criterion in composite design involving triaxial loading, although Criterion B is always more conservative as it includes an additional stress term. In the present study, Criterion B gives a more consistent agreement with the experimental data than Criterion A. Criterion B is also very close to the Weibull longitudinal tensile strength of a small representative volume of 1 mm^3 [16], consistent with failure occurring in a similarly small

volume surrounding the symmetry plane of the specimens. In a plane stress condition or when $\sigma_2 = 0$, Criteria A and B are equivalent.

In an isotropic material, the use of the Tresca stress criterion (Criterion A) implicitly suggests that failure should occur at an angle of 45°, the direction of the maximum shear stress. However, the evidence from the SEM image in Figure 4b shows that the fibres did not fail at a shear angle. It is possible that the very high stress state was confined to a highly localised area such that a macroscopic shear angle could not fully develop. In fact the Tresca stress criterion can be re-interpreted as a deviatoric tensile stress or strain criterion, as done by Sigley et al. [5] to describe tensile failures of glass fibre/polyester at superimposed hydrostatic pressures, which may explain the clean and flat fibre tensile failure surfaces seen in the experiment.

To produce a fibre tensile failure, biaxial compressive transverse stresses are needed for confinement, without which a unidirectional specimen will fail prematurely by either longitudinal splitting or inter-fibre shear at a low transverse compressive stress of about 250 MPa [19] (also shown as a line in Figure 2). At the low transverse stresses that can be withstood by the unidirectional material, the reduction in fibre-direction strength is negligible, allowing non-interactive fibre failure criteria, such as the maximum stress or strain criterion, to be used. The additional constraint provided by the adjacent 90° plies in this work allows the strong interaction between the through-thickness stresses and fibre direction tensile strength to be studied, indicating that the non-interactive fibre dominated failure criteria widely used today for composites need further refinement when the through-thickness stresses are high. Both the fibre failure criteria proposed here are conservative and equally useful for fibre failure stress prediction, with Criterion B performing slightly better for the present tests. More experimental data under triaxial loading of other composite materials is

needed to distinguish better between the two and also to give a better understanding of the mechanism responsible for the stress interaction.

5.0 Conclusion

This study has set out to quantify the interaction between fibre direction tensile stress and through-thickness compressive stress in composite laminates. High transverse compressive stresses can significantly decrease the fibre-direction tensile strength. A biaxial through-thickness compression and longitudinal in-plane tension experiment has been carried out on cross-plied carbon/epoxy specimens. A full range of highly localised through-thickness compressive loads up to the through-thickness compressive strength of the cross-plied laminate has been investigated using indenters of different radii. All specimens failed primarily by a fibre tensile mode. This is made possible by having the 90° plies preventing the 0° plies from early longitudinal splitting. The experiments and the FE analysis both indicated that extremely high local compressive stresses, up to 1700 MPa, could be withstood. Standard failure criteria based on the unidirectional transverse compressive strength of 250 MPa [19] would underestimate the through-thickness compressive strength by a huge margin. Two fibre failure criteria have been proposed, which can be used satisfactorily as conservative criteria for triaxial loading. For a simpler macroscopic laminate based approach, a linear reduction of fibre direction tensile strength as a function of the mean pressure suffices.

Acknowledgement

This work was supported by a Dorothy Hodgkin Postgraduate Award and Rolls-Royce plc. The authors also gratefully acknowledge discussion regarding the SEM fractography with Dr. Emile Greenhalgh from Imperial College London.

References

1. Hinton, M.J., A.S. Kaddour, and P.D. Soden, eds. *Failure Criteria in Fibre Reinforced Polymer Composites: The World-Wide Failure Exercise*. 2004, Elsevier.
2. Hinton, M.J. and A.S. Kaddour, *The background to the Second World-Wide Failure Exercise.* Journal of Composite Materials, 2012. **46**(19-20): p. 2283-2294.
3. Parry, T.V. and A.S. Wronski, *The effect of hydrostatic-pressure on the tensile properties of pultruded CFRP.* Journal of Materials Science, 1985. **20**(6): p. 2141-2147.
4. Parry, T.V. and A.S. Wronski, *The tensile properties of pultruded GRP tested under superposed hydrostatic-pressure.* Journal of Materials Science, 1986. **21**(12): p. 4451-4455.
5. Sigley, R.H., A.S. Wronski, and T.V. Parry, *Tensile failure of pultruded glass-polyester composites under superposed hydrostatic pressure.* Composites Science and Technology, 1991. **41**(4): p. 395-409.
6. Hoppel, C.P.R., T.A. Bogetti, and J.W. Gillespie, *Literature review - Effects of hydrostatic-pressure on the mechanical bahavior of composite materials.* Journal of Thermoplastic Composite Materials, 1995. **8**(4): p. 375-409.
7. Hine, P.J., R.A. Duckett, A.S. Kaddour, M.J. Hinton, G.M. Wells, *The effect of hydrostatic pressure on the mechanical properties of glass fibre/epoxy unidirectional composites.* Composites Part A-Applied Science and Manufacturing, 2005. **36**(2): p. 279-289.
8. Zinoviev, P.A. and S.V. Tsvetkov, *Mechanical properties of unidirectional organic-fiber-reinforced plastics under hydrostatic pressure.* Composites Science and Technology, 1998. **58**(1): p. 31-39.
9. Zinoviev, P.A., S.V. Tsvetkov, G.G. Kulish, R.W. van den Berg, L.J.M.M. Van Schepdael, *The behavior of high-strength unidirectional composites under tension with*

superposed hydrostatic pressure. Composites Science and Technology, 2001. **61**(8): p. 1151-1161.

10. Collings, T.A., *Transverse compressive behaviour of unidirectional carbon fibre reinforced plastics.* Composites, 1974. **5**(3): p. 108-116.
11. Henriksson, A., *Transverse compressive behaviour of carbon-epoxy laminates and its influence on contact laws*, 1990, The Aeronautical Research Institute of Sweden: Stockholm.
12. Wisnom, M.R., S. Jahn, K.W. Gan, S.R. Hallett, *The effect of through-thickness compression on the tensile strength of carbon-fibre composites*, in *25th American Society for Composites Annual Technical Conference*2010: Dayton OH, USA.
13. O'Brien, T.K. and R. Krueger, *Analysis of ninety degree flexure tests for characterization of composite transverse tensile strength.* NASA TM-2001-211227 ARL-TR-2568, 2001.
14. *Hexcel Datasheet.* www.hexcel.com. Accessed on 25 May 2013.
15. Gan, K.W., M.R. Wisnom, and S.R. Hallett, *An approximate model of cylindrical and spherical contact on composite laminates of finite thickness.* Composite Structures, 2013. **103**(0): p. 136-142.
16. Hallett, S.R., B.G. Green, W.G. Jiang, M.R. Wisnom, *An experimental and numerical investigation into the damage mechanisms in notched composites.* Composites Part A-Applied Science and Manufacturing, 2009. **40**(5): p. 613-624.
17. Guo, Y., D. Post, and B. Han, *Thick composites in compression: An experimental study of micromechanical behavior and smeared engineering properties.* Journal of Composite Materials, 1992. **26**(13): p. 1930-1944.
18. Hallett, S.R., W.G. Jiang, B. Khan, M.R. Wisnom, *Modelling the interaction between matrix cracks and delamination damage in scaled quasi-isotropic specimens.* Composites Science and Technology, 2008. **68**(1): p. 80-89.

Published in Composites Science and Technology 90 (2014) 1–8
DOI: 10.1016/j.compscitech.2013.10.010

19. Koerber, H., J. Xavier, and P.P. Camanho, *High strain rate characterisation of unidirectional carbon-epoxy IM7-8552 in transverse compression and in-plane shear using digital image correlation.* Mechanics of Materials, 2010. **42**(11): p. 1004-1019.

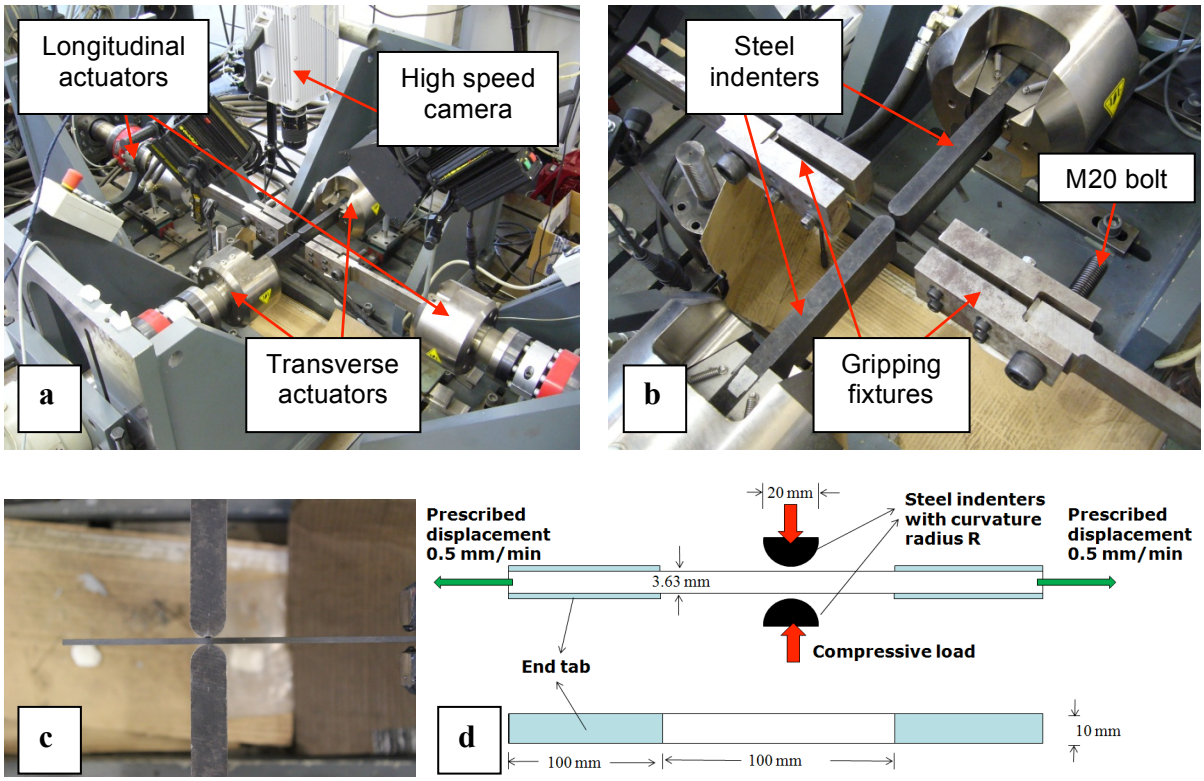

Figure 1: (a) Overview of biaxial actuator positioning and the high speed camera. (b) Details of test configuration. (c) Pure through-thickness compression loading with indenters of radius of curvature R = 10 mm. (d) Specimen with its dimensions used in the biaxial testing.

Published in Composites Science and Technology 90 (2014) 1–8
DOI: 10.1016/j.compscitech.2013.10.010

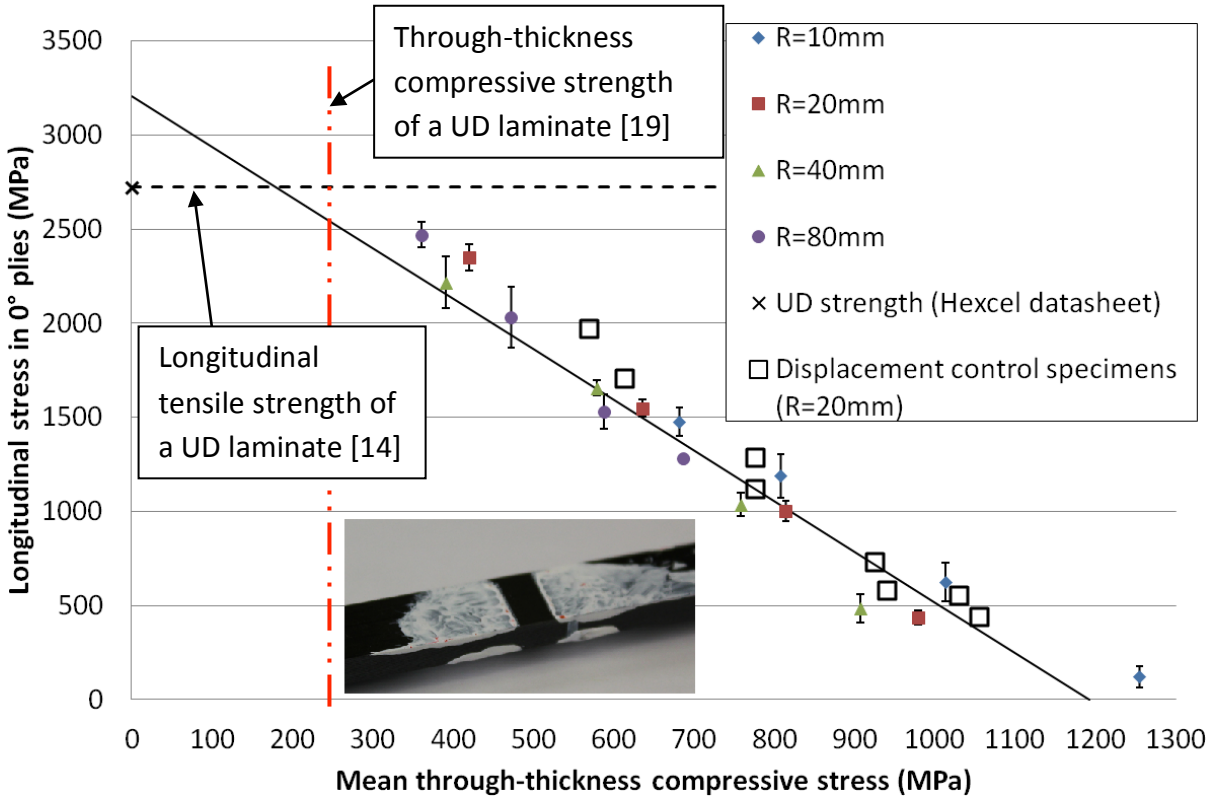

Figure 2: Failure envelope of IM7/8552 carbon/epoxy cross-plies subjected to biaxial through-thickness compression and in-plane tension. (Inset: The mean through-thickness compressive stresses were calculated based on the contact area as marked by the absence of white paint.)

Published in Composites Science and Technology 90 (2014) 1–8
DOI: 10.1016/j.compscitech.2013.10.010

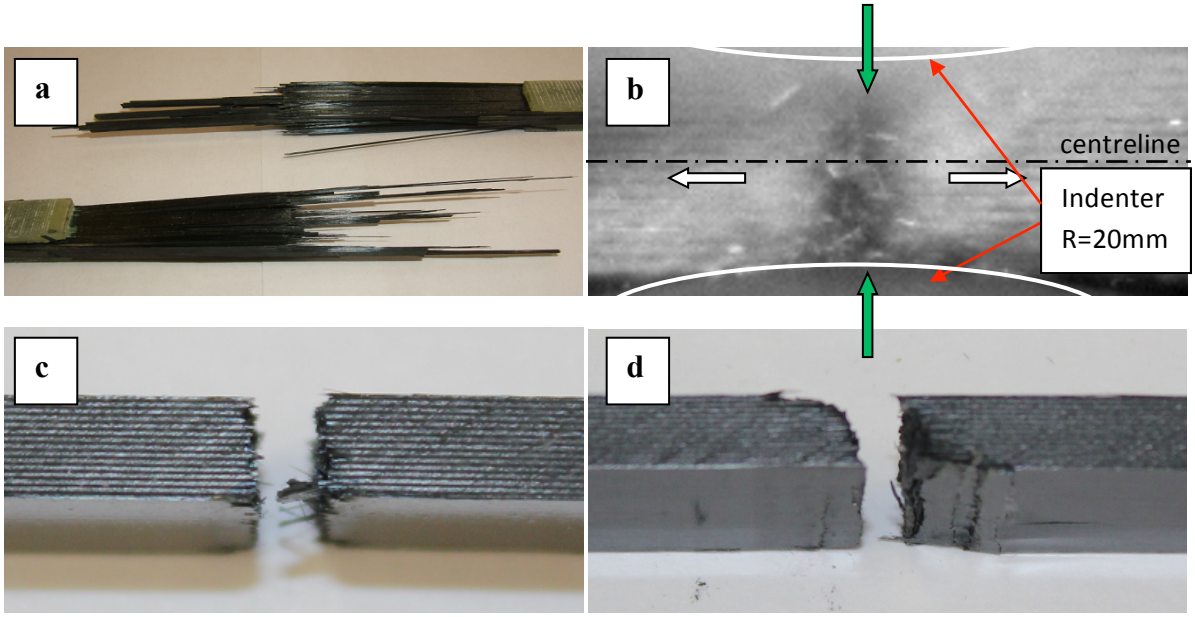

Figure 3: Failure of biaxially loaded specimens with indenters R = 20 mm. (a) Longitudinal splitting of fibres in a unidirectional specimen 12.5 kN through-thickness (TT) compression load case, load control. (b) High speed camera image of a cross-ply specimen in 25 kN TT compression load case, in load control, showing the specimen failed on a vertical symmetry plane. Fracture surface of a cross-ply specimen in (c) low 17.6 kN TT compression and (d) high 50.3 kN TT compression load cases, displacement control.

Published in Composites Science and Technology 90 (2014) 1–8
DOI: 10.1016/j.compscitech.2013.10.010

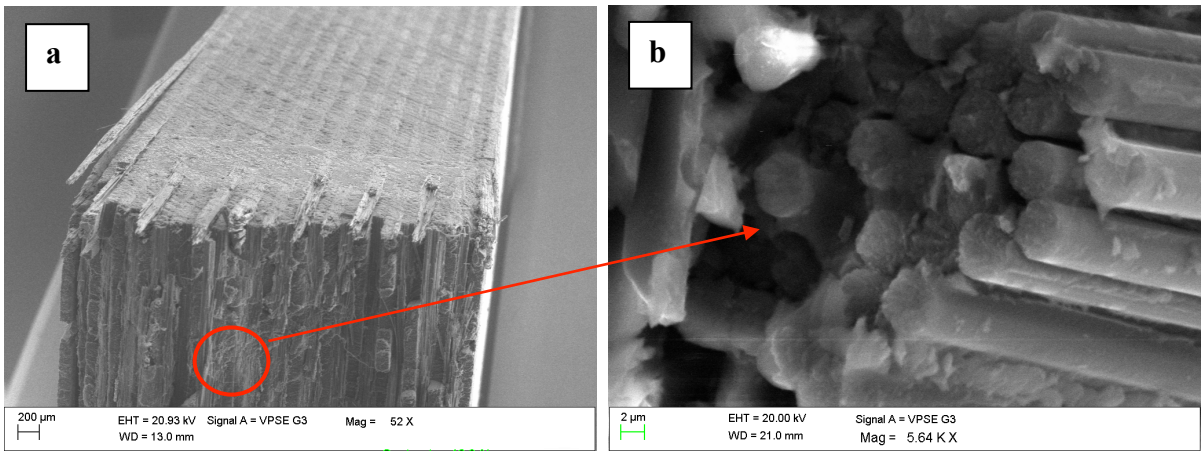

Figure 4: (a) A SEM image of the fracture surface of a specimen failed purely by through-thickness compression loading. (b) Tensile fibre fracture mode.

Published in Composites Science and Technology 90 (2014) 1–8
DOI: 10.1016/j.compscitech.2013.10.010

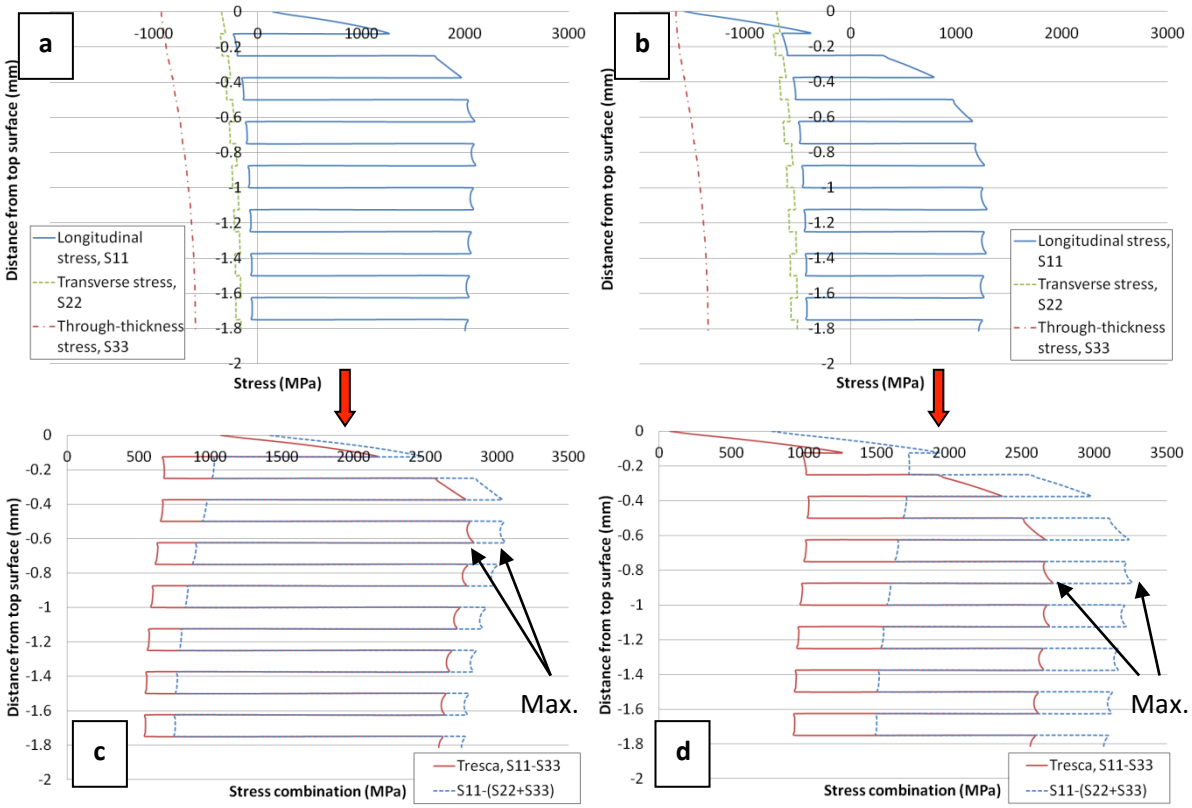

Figure 5: Principal stress distributions at failure on the failure plane in load cases (a) indenter R = 10 mm, through-thickness compression 15 kN, longitudinal tensile load 28.4 kN and (b) indenter R = 10 mm, through-thickness compression 40 kN, longitudinal failure tensile load 2.3 kN. Stress combinations which constitute two different failure criteria are shown in (c) and (d) for the two cases respectively. (Note: Zero distance refers to the top surface.)

Published in Composites Science and Technology 90 (2014) 1–8
DOI: 10.1016/j.compscitech.2013.10.010

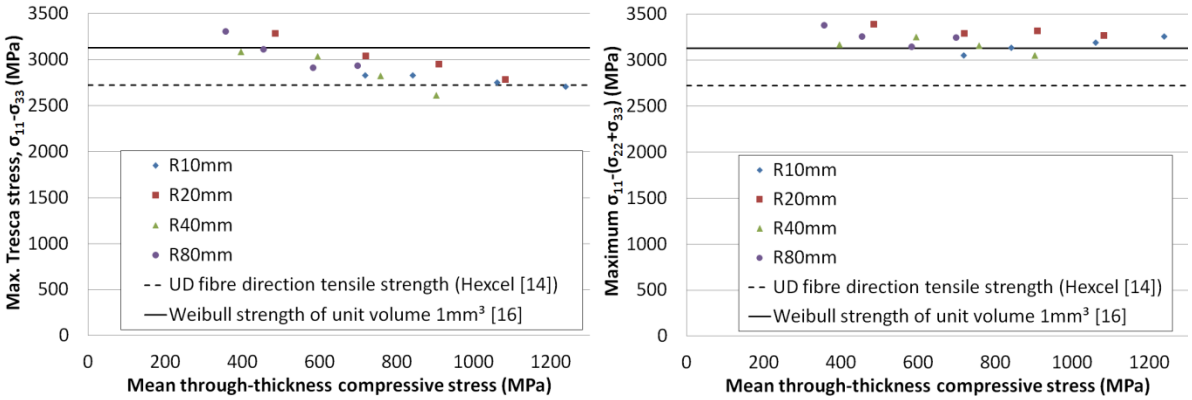

Figure 6: The maximum combined stresses (left) [σ_{11}-σ_{33}] and (right) [σ_{11}-(σ_{22}+σ_{33})] of all biaxial load cases fall above the nominal unidirectional fibre-direction tensile strength.

Published in Composites Science and Technology 90 (2014) 1–8
DOI: 10.1016/j.compscitech.2013.10.010

Table 1: Experimental results of IM7/8552 carbon/epoxy cross-plies subjected to biaxial through-thickness compression and in-plane tension.

No. of specimens	Through-thickness compressive load (kN)	Contact length, 2*a* (mm)	Longitudinal tensile failure load (kN) (c.v.)
R = 10 mm (Average specimen actual width = 9.6 mm)			
3	15	2.29	28.4 (4.4%)
4	20	2.59	22.7 (6.5%)
4	30	3.09	11.9 (11.7%)
4	40	3.33	2.3 (44.7%)
R = 20 mm (Average specimen actual width = 9.9 mm)			
4	12.5	3.00	46.5 (2.4%)
5	25	3.99	30.5 (3.0%)
5	37.5	4.65	19.8 (5.3%)
4	50	5.15	8.6 (9.8%)
R = 40 mm (Average specimen actual width = 9.6 mm)			
5	15	4.01	42.3 (3.8%)
5	30	5.43	31.6 (2.8%)
5	45	6.23	19.7 (5.7%)
4	60	6.91	9.2 (13.0%)
R = 80 mm (Average specimen actual width = 9.8 mm)			
3	20	5.68	48.1 (2.6%)
5	30	6.53	39.5 (4.7%)
5	45	7.85	29.8 (4.6%)
4	60	8.95	25.0 (2.3%)